The Structure of a $T = 1$ Icosahedral Empty Particle from Southern Bean Mosaic Virus

John W. Erickson, Abelardo M. Silva, M. R. N. Murthy, Ignacio Fita, Michael G. Rossmann

Abstract. *The structure of a* T = *1 icosahedral particle (where* T *is the triangulation number), assembled from southern bean mosaic virus coat protein fragments that lacked the amino-terminal arm, was solved by means of model building procedures with the use of 6-angstrom resolution x-ray diffraction data. The icosahedral five-, three-, and twofold contacts were found to be similar, at this resolution, to the analogous contacts (icosahedral five-, quasi-three-, and quasi-twofolds) found in the parent* T = *3 southern bean mosaic virus. However, the icosahedral fivefold contacts of the* T = *3 structure are the most conserved in the* T = *1 capsid. These results are consistent with a mechanism in which pentameric caps of dimers are the building blocks for the assembly of* T = *1 and* T = *3 icosahedral viruses.*

The eight-stranded antiparallel β barrel (Fig. 1) (*1*) is a common structural theme among some $T = 1$ and $T = 3$ (where T is the triangulation number as defined by Caspar and Klug (*2*)) icosahedral RNA plant viruses, such as satellite tobacco mosaic virus (*3*) (STNV), southern bean mosaic virus (*4*) (SBMV), tomato bushy stunt virus (*5*) (TBSV), and turnip crinkle virus (TCV) (*6*). Nevertheless, the subunit packing arrangement in STNV, a $T = 1$ virus, differs markedly from that in the $T = 3$ viruses, SBMV, TBSV, and TCV. This difference may be a consequence of different amino acids in subunit contact regions or different icosahedral constraints in $T = 1$ and $T = 3$ particles.

SBMV coat protein subunits (28,214 daltons) will assemble with either viral RNA or transfer RNA (tRNA) into $T = 3$ or $T = 1$ nucleoprotein particles (*7*). The amino-terminal 61 residues of the coat protein can be removed by trypsin to yield a 22,000-dalton fragment (P22), which readily assembles into $T = 1$ shells in the absence of RNA (*8*). These $T = 1$ particles crystallize in the cubic space group $P2_13$, with $a = 247.0$ Å. The crystals permitted us to determine whether the P22 subunit, with a sequence identical to that of the native SBMV coat protein, would pack with a subset of the SBMV $T = 3$ contacts or with an alternative packing scheme, as in STNV $T = 1$. Hence, this study provides information on the important protein interaction required in the assembly of viral capsids.

The 180 chemically identical subunits in the SBMV $T = 3$ capsid are distributed among three, quasi-equivalent environments—designated A, B, and C—to form several distinct types of contacts (*9*) (Fig. 2). Subunits are related by (i) icosahedral fivefold axes, I5, creating the contacts AA_5; (ii) quasi-threefold axes, Q3, creating the AB, BC, CA contacts; (iii) quasi-twofold axes, Q2, creating the AB_5 contacts; (iv) icosahedral-twofold axes, I2, creating the CC_2 contacts; (v) quasi-sixfold axes, Q6, creating the CB_5 and B_2C contacts, as well as the β-annulus CC_3 contacts.

Of the two types of quasi-sixfold contacts (B_2C and CB_5), only B_2C is unlike any other type of contact, whereas the CB_5 contact is essentially identical to the AA_5 contact. The two types of twofold contacts, AB_5 and CC_2, differ principally by the insertion of the βA arms (Fig. 1) in the interface between the two C subunits. This arm is disordered in the A and B subunits and corresponds exactly to that portion cleaved from the native SBMV subunit to produce the P22 fragment. Thus, the $T = 1$ capsid of P22 might be assembled with pentamers, trimers, or AB_5 dimers found in the $T = 3$ capsid. However, of these oligomers only the pentamer can be conserved exactly in the $T = 1$ particles as neither the AB_5 dimer nor the ABC trimer are related by exact icosahedral symmetry. The structure of the crystalline SBMV $T = 1$ particle was solved at 6-Å resolution, with the use of model building procedures, based on a rigid SBMV subunit as found in the native virus.

X-ray data collection. CuKα x-rays were produced by an Elliott rotating anode x-ray generator and were focused with double mirrors (*10, 11*). Crystals were mounted with their $(01\bar{1})$ axis along the spindle of a Nonius oscillation camera (*12, 13*). The $\phi = 0°$ setting was defined by placing a (100) axis along the x-ray beam. The crystals were oscillated through 1.5° for each photograph, and successive oscillations were overlapped by 0.3°. A total of 15 oscillation films was collected and used in the range $\phi = 0°$ to 18°. In general, two data films were obtained from a single crystal by translating the crystal to a different position in the x-ray beam between exposures. The films were processed according to procedures developed by Rossmann (*14*) and Rossmann *et al.* (*15*). The overall agreement of 13,538 common intensities obtained from 25,889 reflections on different films was 14.9 percent for all data from ∞ to 4.5 Å with $F^2 \geq 1\sigma$. The high R factor (*16*) reflects the relatively weak intensity data that were collected at higher resolution (7.5 to 4.5 Å) (Table 1).

Particle packing and orientation. Erickson and Rossmann (*8*) reported that the crystals of $T = 1$ SBMV particles exhibited $m3$ Laue symmetry and assigned them to space group $P23$. However, on reexamination of the diffraction data the space group was found to be $P2_13$. This space group requires that there are four particles, placed on crystallographic threefold axes, at (x,x,x), $(\bar{x}+½,\bar{x},x+½)$, $(\bar{x},x+½,\bar{x}+½)$, and $(x+½,\bar{x}+½,\bar{x})$. When x equals either 0 or ¼, a uniform, close-packed arrangement of particles will occur. The particles will have a rotational degree of freedom about the crystal threefold axes. However, particles with icosahedral symmetry will form symmetrical contacts in the unit cell only when icosahedral twofold axes are either parallel to the crystallo-

The authors are members of the Department of Biological Sciences, Purdue University, West Lafayette, Indiana 47907. The present address of J. W. Erickson is Abbotts Laboratory, Department of Pharmaceutical Discovery, Abbott Park, Illinois 60064. The present address of A. M. Silva is Departamento de Física, Facultad de Ciencias Exactas, Universidad Nacional de La Plata, C.C. No. 67, 1900 La Plata, Argentina. The present address of M. R. N. Murthy is Molecular Biophysics Unit, Indian Institute of Science, Bangalore 560012, India.

Table 1. Percentage of observed data as a function of resolution shell.

Resolution	n^* ($F^2 \geq 1\sigma$)	Percentage of theoretically possible	
		$F^2 \geq 1\sigma$	$F^2 \geq 2\sigma$
∞–30.0	55	57	39
15.0–30.0	534	78	70
10.0–15.0	1426	77	69
7.5–10.0	2512	70	53
5.0–7.5	6528	44	22
4.5–5.0	2483	6	3

*Number of measurements.

graphic axes or parallel to the unit cell face diagonals. The first orientation will be defined by $\phi = 0°$ and the second orientation is attained by rotation of the particles by 82.24° about the crystallographic threefold axes. The former case was observed approximately for the packing in rhinovirus $P2_13$ crystals ($\phi = -6.0°$) (*12*). The latter case was observed approximately for Mengo virus ($\phi = 82.3°$) (*13*). When $\phi = 82.24°$, there exists a fourfold relation between the particle orientations. This fourfold property extends only to producing similar particle orientations, not to superimposing them in space. That is, the fourfold property is valid only for the self-vectors within the particle in a Patterson diagram but not for the cross-vectors.

A self-rotation function (*17*) with data between 15-Å to 7-Å resolution, showed the presence of fourfold peaks along crystal axes, and twofold peaks along positions corresponding to face diagonals of the unit cell. These peaks were one-third to one-half as high as the origin peaks, suggesting a particle orientation near $\phi = 82.24°$. A locked rotation function (*12, 18*) was computed to determine the precise particle orientation. An icosahedron, placed on a crystal threefold axis, was rotated about that axis by ϕ. For each value of ϕ, the rotation function value was computed at all independent icosahedral axes. These values were then summed and plotted as a function of ϕ (Fig. 3). The larger peak at $\phi = 44°$ corresponds to the coincidence of crystal two- and threefold axes with particle twofold and threefold axes. The peak at 81.5° gives the actual particle orientation, which deviates by only 0.7° from the orientation required to produce a fourfold relationship between the particle orientations. Given the orientation and approximate position ($x = 0$ or $x = \frac{1}{4}$) of each of the four particles in the unit cell, as well as the known $T = 3$ SBMV structure, it was then possible to build trial structures of the $T = 1$ SBMV capsid into the unit cell.

Model building and refinement. SBMV $T = 1$ atomic models were computed with the atomic coordinates of the A subunit obtained from the refined SBMV $T = 3$ native structure (*19*). The starting assumption was that the $T = 3$ AA_5 pentamer, or the ABC trimer, or the AB_5 dimer would be conserved in the $T = 1$ structure (Fig. 2). Therefore, each of these oligomers were used to construct different starting models in which

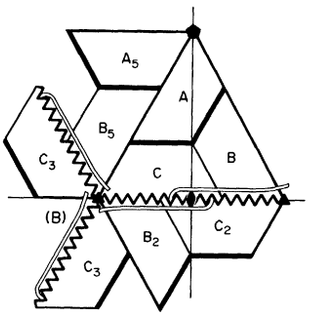

Fig. 2. Arrangement of the quasi-equivalent A, B, and C subunits within one icosahedral asymmetric unit of a $T = 3$ SBMV particle and the right-handed coordinate system P,Q,R to which all atomic positions are referred.

the $T = 3$ symmetry axis (I5, Q3, or Q2) was superimposed onto the corresponding $T = 1$ symmetry axis (I5, I3, or I2, respectively). The radius, r, of the particle was chosen to avoid significant overlap between subunits within the $T = 1$ capsid while yet retaining some contacts between subunits. The dimer, trimer, or pentamer were then systematically rotated by an angle, τ, about the corresponding symmetry axis. This rotation will preserve one type of contact and alter the other two. For example, rotation of the pentamer by τ about the fivefold axis will alter the contacts between twofold and threefold related subunits. The complete particle could then be generated by icosahedral symmetry and placed at (x,x,x) onto a threefold axis in the unit cell, rotated by $\phi = 81.5°$, and operated on by the space group symmetry to generate the other three particles. Thus, only three parameters were varied for the three $T = 1$ models: the radius, r; the rotation, τ (Fig. 4); and the translation, x.

The models were tested by computing structure factors (F_{calc}) and comparing these with the observed structure amplitudes in terms of the conventional R factor

$$\left(R = \frac{\Sigma|(|F_{obs}| - |F_{calc}|)|}{\Sigma|F_{obs}|}\right)$$

The calculations were performed on a Cyber 205 computer with a vectorized algorithm. In order to save computing time only every second reflection between 12-Å and 6-Å resolution and with $F^2 \geq 3\sigma$ was selected for this purpose, giving a total of 1342 observed structure factors.

An example of an R-factor search over r and τ at $x = 0$ in which the AA_5 pentamer is conserved is presented in Fig. 5. The search displayed a deep minimum at $r = 77$ Å, $\tau = -36°$, and $x = 0°$. This position and orientation for the pentamer corresponded to a model in which the

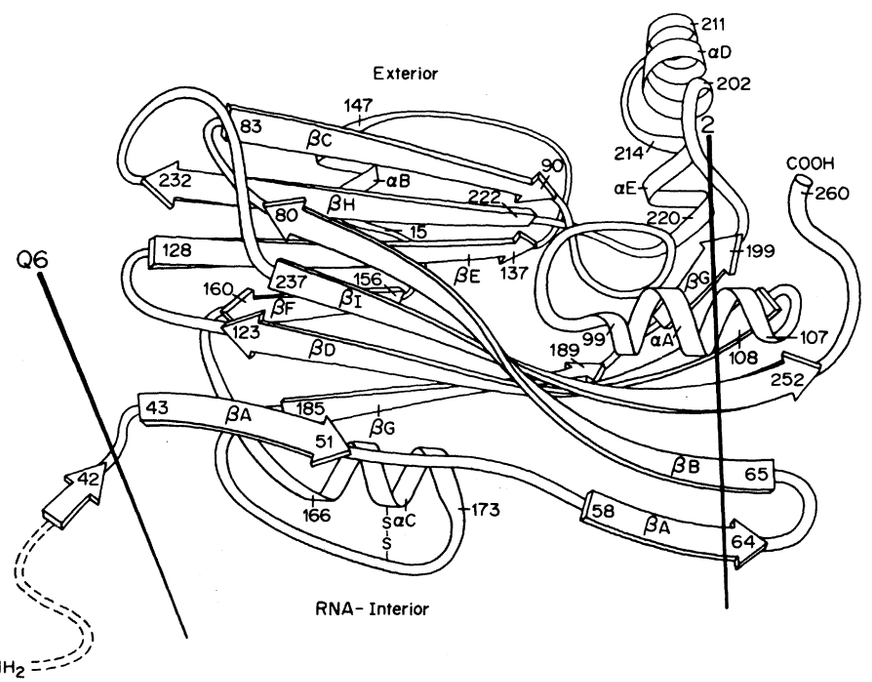

Fig. 1. Diagrammatic representation of subunit C of SBMV coat protein. The amino-terminal βA arm is absent in the modified subunit used to assemble the $T = 1$ particle.

trimer and dimer would mimic the ABC trimer and AB_5 dimer in the $T = 3$ capsid. The particle orientation (ϕ) and position (x) could then be further refined by R-factor minimization based on the best pentamer model. The particle center changed by 0.4 Å to $x = 0.001$, and ϕ changed by 0.35° to 81.15°, for all three starting models. Identical results were obtained with all reflections between 12-Å and 6-Å resolution with $F^2 \geqq 2\sigma$ (4434 reflections). The R-factor minimum for the pentamer model (30.9 percent) was about 0.8 percent less than that obtained for either the dimer or trimer models (31.7 percent). Thus, approximate conservation of the AB_5 dimer or ABC trimer leads to a somewhat poorer solution of the SBMV $T = 1$ crystal structure than does exact conservation of the AA_5 pentamer.

The subunit position and orientation for each of the three models was optimized further by a rigid body R-factor minimization. The subunit was released from retaining the twofold, threefold, or fivefold $T = 3$ contacts that had been assumed previously. Small rotations and translations were applied to the subunit. The small rotations were expressed as Eulerian angles θ_1, θ_2, θ_3 [see (*17*) for the definition]. Because of the special symmetry when θ_2 is small, the exploration was performed in course intervals of $(\theta_1 - \theta_3)$ for small values of $(\theta_1 + \theta_3)$. The search covered the ranges $0 \leqq \theta_2 \leqq 4.5°$ in initial intervals of 1.5° and final intervals of 0.5°, $-4.5 \leqq (\theta_1 + \theta_3) \leqq 4.5°$ in initial intervals of 1.5° and final intervals of 0.5°, and $0 \leqq (\theta_1 - \theta_3) < 360°$ in initial intervals of 45°, decreasing to 20° and finally to 2°. The search did not cover every point within these ranges, but was a stepwise procedure to determine the angles that resulted in the lowest R factors. The process appeared to be path-independent.

The best values of the small translation, t, of the SBMV subunit were determined initially by exploring x, y, and z in 0.25-Å intervals. These values were then used to refine the Eulerian angles. This translation-rotation procedure converged in two or three cycles to around $R = 29$ percent in all cases (Table 2). The overall R factor decreased 2.3 percent for the initial dimer and trimer models and 1.5 percent for the initial pentamer model. Finally, another check was made on the position and orientation of the particle; no further changes were observed. The root-mean-square (rms) distance between the alpha-carbon (C_α) atoms of the initial models ranged from 0.86 to 1.23 Å; however, the rms distance between the C_α atoms of the final models decreased to less than 0.15 Å (Table 3). Thus, all three starting models had converged to a common structure. The model based on the conservation of the $T = 3$ SBMV pentamer produced the smallest subunit movement (rms distance of 0.48 Å) during the rigid body refinement.

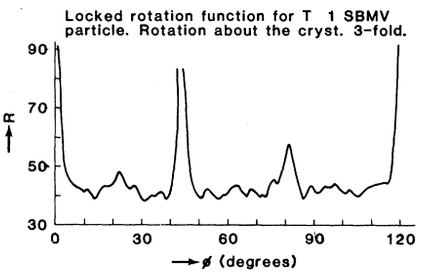

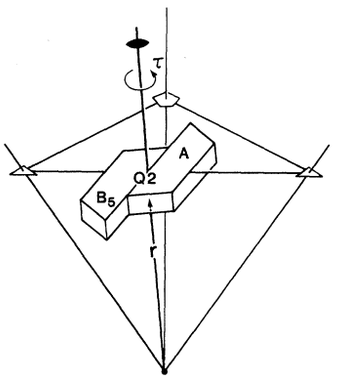

Fig. 3 (left). The locked rotation function for $T = 1$ SBMV obtained by rotating an icosahedron about the crystal threefold axes. Fig. 4 (right). Diagram showing parameters used in building models of the $T = 1$ SBMV capsid. In this example, the AB_5 (Q2) dimer has been taken from the $T = 3$ SBMV structure and superimposed onto the $T = 1$ icosahedral twofold axis. The parameters which can be varied are τ, the rotation of the AB_5 dimer about the twofold axis, and r, a measure of the radial distance of the dimer from the particle center.

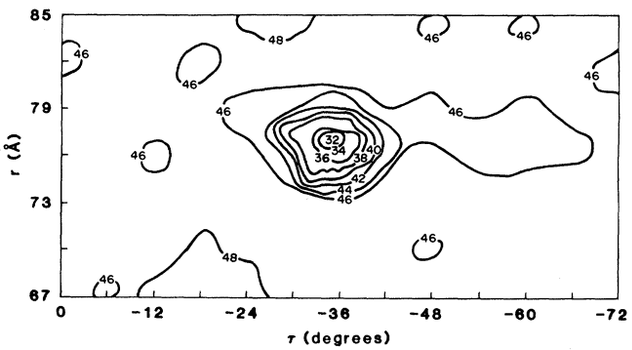

Fig. 5. R factors obtained by using an AA_5 pentamer from the native $T = 3$ SBMV structure in constructing the $T = 1$ SBMV capsid. The radial distance r is the distance between an arbitrary point in the A subunit from the $T = 1$ capsid center. The rotation of the pentamer about the $T = 1$ icosahedral fivefold axis is given by τ. The search therefore repeats itself after 72°. The $\tau = \pm 36°$ orientation will place the $T = 3$ SBMV Q2 and Q3 axes closest to the $T = 1$ SBMV I2 and I3 axes. The particle center was assumed to be at $x = 0.0$, with an orientation of $\phi = 81.5°$ about the crystallographic threefold axis.

Table 2. Rigid body search results. The R factor was computed on the basis of 1342 reflections, with $F^2 > 3\sigma_F$ in the 12.0 to 6.0 Å resolution range. The rigid body parameters were computed with $r = 76$ Å for the pentamer model.

Starting model	R (%)		Å			Eulerian angles (°)		
	Initial	Final	t_x	t_y	t_z	θ_2	$\theta_1 + \theta_3$	$\theta_1 - \theta_3$
Pentamer	30.9	29.4	−0.15	−0.35	0.80	1.5	1.0	329.0
Trimer	31.7	29.5	0.45	−0.05	−0.15	2.0	1.5	358.5
Dimer	31.7	29.4	0.35	0.05	0.05	2.5	−2.0	32.0

Table 3. The rms distances in angstroms between equivalent C_α atoms within one subunit for various models before and after rigid body refinement. Abbreviations: PS, pentamer starting (before Eulerian search); PF, pentamer final (after Eulerian search); TS, trimer starting; TF, trimer final; DS, dimer starting; and DF, dimer final.

	PS	TS	DS	PF	TF	DF
PS		1.23	1.03	0.48	0.55	0.52
TS			0.86	0.87	0.81	0.83
DS				0.74	0.78	0.79
PF					0.15	0.13
TF						0.12
DF						

Table 4. Differences in the distance between C_α positions separated by less than 7 Å in the subunit interfaces of $T = 1$ and $T = 3$ capsids.

Model	Differences (Å)*								
	Pentamer contacts			Trimer contacts			Dimer contacts		
	rms	Mean	n	rms	Mean	n	rms	Mean	n
Pentamer starting	0.00	0.00		0.62	−0.49	24	0.45	0.06	19
Final	0.23	−0.09	39	0.38	−0.07	24	0.49	−0.10	19

*Definitions: Let d_3 be the distance between two C_α atoms in adjoining subunits in the $T = 3$ capsid. Let d_1 be the corresponding distance in the $T = 1$ capsid.

Then the rms difference = $\sqrt{\sum^{n} (d_3 - d_1)^2/n}$ and the mean difference = $\sum^{n} (d_3 - d_1)/n$ where n is number of close C_α approaches with $d_3 \leq 7$ Å.

A $(2F_{obs} - F_{calc})$ difference electron density map to 5.0-Å resolution was calculated, based on phases and values of F'_{calc} derived from the final model. This map did not indicate any significant structural changes of the A subunit. In addition, the five-, three-, and twofold contact regions of the $T = 1$ model closely resemble the I5-, Q3-, and Q2-fold $T = 3$ contacts insofar as visual inspection allowed. In particular, the Ca^{2+}-binding sites and carboxylate clusters in the threefold contacts have been preserved in the SBMV $T = 1$ structure.

The final coordinates of the SBMV $T = 1$ particle can be generated from the refined A subunit coordinates of the $T = 3$ SBMV structure (deposited with the Brookhaven Protein Data Bank) in the following steps.

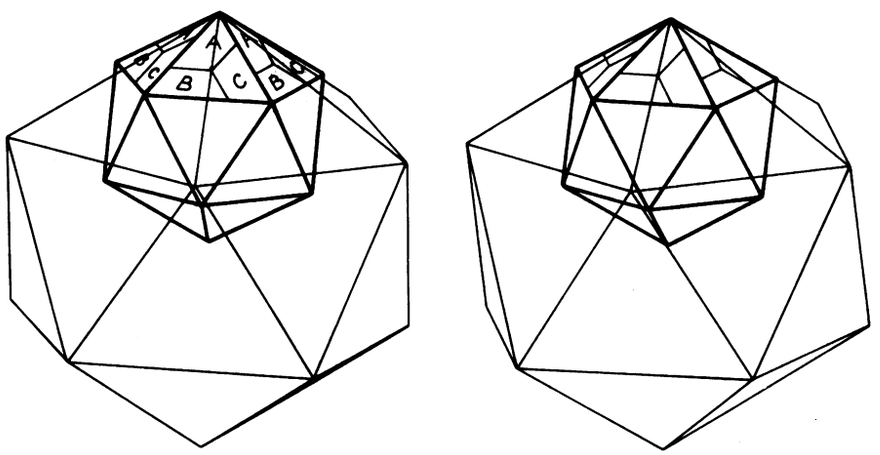

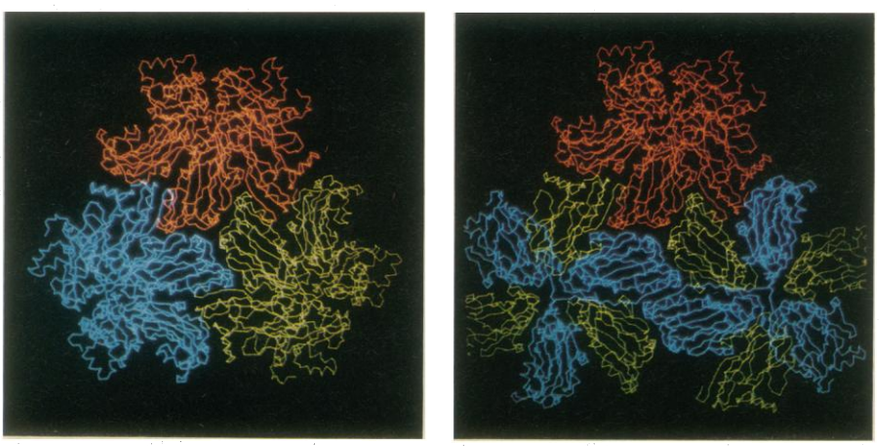

Figs. 6 to 8. The $T = 1$ and $T = 3$ capsids have common pentadecamer caps. However, they differ in how the caps are associated with each other. Fig. 6 (top). Stereodiagram showing outline of superimposed $T = 1$ and $T = 3$ icosahedrons with common pentadecamer cap. Fig. 7 (bottom left). View down the threefold axis showing polypeptide fold in $T = 1$ particle. Fig. 8 (bottom right). View down the threefold axis as in Fig. 7 but showing polypeptide folds for the native $T = 3$ particle.

1) Position the A subunit by means of the operation:

$$P' = \begin{pmatrix} 0.8156 & 0.4842 & 0.3169 \\ -0.4935 & 0.8679 & -0.0561 \\ -0.3022 & -0.1107 & 0.9468 \end{pmatrix} P + \begin{pmatrix} -1.0 \\ 32.8 \\ -56.2 \end{pmatrix}$$

where P are the refined coordinates of the A subunit atoms referred to the P, Q,R system of the $T = 3$ particle (Fig. 3) and P' are the coordinates of the A subunit atoms in the $T = 1$ SBMV particle placed at the origin of the P,Q,R system with its icosahedral axes coincident to those of the larger $T = 3$ particle. The icosahedral symmetry axes in the $T = 3$ system can then be used to generate the other 59 subunits of the $T = 1$ particle. Orthogonal icosahedral twofold axes are defined as being along the P,Q,R axes of the $T = 3$ system as shown in Fig. 2.

2) The particle is then positioned and oriented in the $T = 1$ SBMV cell by the operation:

$$P'' = \begin{pmatrix} 0.8525 & -0.2884 & 0.4359 \\ 0.4359 & 0.8525 & -0.2884 \\ -0.2884 & 0.4359 & 0.8525 \end{pmatrix} P' + \begin{pmatrix} 0.2 \\ 0.2 \\ 0.2 \end{pmatrix}$$

which represents a translation along and rotation about the crystallographic threefold axis. The other four particles in the $T = 1$ SBMV cell can then be generated by the 2_1 crystallographic axes.

Comparison of subunit contacts in the T = *1 and* T = *3 capsids*. The similarity between subunit contacts in the $T = 1$ and $T = 3$ capsids was assessed by comparing the distances between C_α atoms separated by less than 7 Å across subunit interfaces (Table 4). The 7-Å limit was chosen to restrict the comparison to residues in the interface without making any assumptions about the exact position of side chain atoms in the $T = 1$ structure.

The $T = 3$ pentamer, trimer, and dimer contacts are all preserved to within 0.5-Å rms deviation in the $T = 1$ SBMV capsid. The degree of preservation is roughly proportional to the number of close $C_\alpha - C_\alpha$ approaches in the interface, with the pentamer contacts being the most preserved. The rigid body refinement of the pentamer model increased the similarity between the trimer contacts in the $T = 1$ and $T = 3$ capsids, at the cost of destroying exact conservation of the pentamer contacts. The dimer contacts were less affected by the refinement. Hence, the main effect of the rigid body refinement of the pentamer starting model was to reduce the distances between subunits at the threefold interface. The degree of preservation of the contacts might be even higher if there were a slight distortion of the SBMV subunit

which cannot be detected at the resolution of this study.

Discussion. The model building analysis to 5-Å resolution of the $T = 1$ SBMV capsids of P22 shows that the AA_5 pentamer contacts, present in the $T = 3$ native SBMV structure, are the most closely maintained in the $T = 1$ capsids. The ABC trimer and AB_5 dimer contacts are also conserved but to a lesser extent. If the pentamer contacts were exactly conserved then there would be an increase in the gap between subunits of the trimer clusters. This, however, is not the case. Rather, the pentamer and timer contacts are maintained at the cost of the preservation of the dimer and, to a lesser extent, the trimer contacts. From a geometrical point of view, a $T = 3$ SBMV capsid can be considered as being composed of 12 pentadecamer units which are quasi-equivalent to a portion of the $T = 1$ capsid (Fig. 6). However, the interrelationships of the pentadecamer in the $T = 3$ capsids are quite different to those in the $T = 1$ capsid (Figs. 7 and 8).

The similarity of subunit contacts in the $T = 1$ and $T = 3$ SBMV particles shows that these capsids are primarily stabilized by protein-protein interactions and also explains the similar *p*H and Ca^{2+} ion requirements for their assembly (*7*). The maintenance of the Ca^{2+} sites between subunits of the trimer clusters (*9*) in the $T = 1$ structure probably provides the driving force for the observed relative distortion between the common interactions of the $T = 1$ and $T = 3$ capsids. The character of the protein-protein interactions can be modified by *p*H and Ca^{2+} levels: $T = 1$ capsids are favored at *p*H 5 to 7; $T = 3$ capsids are favored at *p*H 7 to 8. The role of the viral RNA in assembly is less clear. It is required as a nucleating agent for intact coat protein but not for P22, implying that neutralization of the basic amino-terminal arm is essential for assembly. Rossmann *et al.* (*9*) postulated the existence of a pentameric cap formed from dimers, and this is consistent with the greater conservation of pentamer contacts which was observed for $T = 1$ and $T = 3$ particles. These contacts must be formed at an early stage in assembly from dimers of SBMV coat protein or P22, both of which have been observed in solution (*20*). While the structure of these dimers is unclear, the exact nature of the two- and threefold contacts in the assembled icosahedrons depends upon the resultant charge state of the carboxylate clusters in the threefold contact regions. These clusters serve as switches to regulate capsid assembly and disassembly for both types of particles (*7*). Thus, the $T = 1$ and $T = 3$ structures conserve not only most of their subunit contacts but also their regulatory mechanisms for assembly and disassembly.

Rossmann *et al.* (*9*) and Rossmann (*21*) proposed that dimers are essential building blocks in the assembly of $T = 3$ viruses, in which quasi-equivalent contacts can be achieved from two alternative bonding arrangements for the dimer (AB_5 and CC_2 for SBMV and TBSV $T = 3$ particles). These different arrangements are the consequence of malleable dimer contacts. The greater flexibility of dimers, in contrast to the trimers and pentamers (Table 4), is a consequence of the small number of interactions. Hence, a dimer useful in the assembly of a $T = 3$ particle should also be suitable for a $T = 1$ particle. This argument is not necessarily true if the dimer contacts are extensive, which would preclude the alternative quaternary structures, as in the case of STNV (*3*). Hence, the existence of a highly stable dimer might preclude assembly of $T = 3$ capsids.

Ionizable switches in the SBMV dimer contacts would lock the dimer into a given state prior to assembly, precluding the possibility of a quaternary structural change during assembly. However, the existence of these switches in the threefold contacts implies that their state must be communicated across at least 12.6 Å, corresponding to the distance of the Ca^{2+} ion sites from their closest twofold axes. In short, the control of the assembly into capsids of different geometries is determined by the communication of the state of charge of the carboxyl clusters in the trimers to effect the mode of successive addition of the malleable dimers.

References and Notes

1. M. G. Rossmann *et al.*, *J. Mol. Biol.* **165**, 711 (1983).
2. D. L. D. Caspar and A. Klug, *Cold Spring Harbor Symp. Quant. Biol.* **27**, 1 (1962).
3. L. Liljas, T. Unge, T. A. Jones, K. Feisborg, S. Lövgren, U. Skoglund, B. Strandberg, *J. Mol. Biol.* **159**, 93 (1982).
4. C. Abad-Zapatero *et al.*, *Nature (London)* **286**, 33 (1980).
5. S. C. Harrison, A. J. Olson, C. E. Schutt, F. K. Winkler, G. Bricogne, *ibid.* **276**, 368 (1978).
6. S. C. Harrison, *Trends Biochem. Sci.* **9**, 345 (1984).
7. H. S. Savithri and J. W. Erickson, *Virology* **126**, 328 (1983).
8. J. W. Erickson and M. G. Rossmann, *ibid.* **116**, 128 (1982); J. H. Tremaine and W. P. Ronald, *ibid.* **91**, 164 (1978).
9. M. G. Rossmann, C. Abad-Zapatero, M. A. Hermodson, J. W. Erickson, *J. Mol. Biol.* **166**, 37 (1983).
10. S. C. Harrison, *J. Appl. Crystallogr.* **1**, 84 (1968).
11. A. Francks, *Proc. Phys. Soc. London Ser. B* **68**, 1054 (1955).
12. E. Arnold *et al.*, *J. Mol. Biol.* **177**, 417 (1984).
13. M. Luo *et al.*, *ibid.* **180**, 703 (1984).
14. M. G. Rossmann, *J. Appl. Crystallogr.* **12**, 225 (1979).
15. ———, A. G. W. Leslie, S. S. Abdel-Meguid, T. Tsukihara, *J. Appl. Crystallogr.* **12**, 570 (1979).
16. The agreement was defined as

$$R = \frac{\sum_h \sum_i |(F_h^2 - F_{hi}^2)|}{\sum_h \sum_i F_h^2} \times 100$$

where F_h^2 is the mean of the i intensity observations F_{hi}^2 of reflection h.
17. M. G. Rossmann and D. M. Blow, *Acta Crystallogr.* **15**, 24 (1962).
18. M. G. Rossmann, G. C. Ford, H. C. Watson, L. J. Banaszak, *J. Mol. Biol.* **64**, 237 (1972).
19. A. M. Silva and M. G. Rossmann, *Acta Crystallogr.* **B41**, 147 (1985).
20. J. W. Erickson and B. J. M. Verduin, unpublished data.
21. M. G. Rossmann, *Virology* **134**, 1 (1984).

22. We thank Ming Luo for help in performing some of the rotation function calculations and Sharon Wilder for help in the preparation of this manuscript. Supported by grants from the U.S. Department of Agriculture, National Science Foundation, and National Institutes of Health.

6 May 1985; accepted 11 July 1985